

UCRL 2708

UNCLASSIFIED

UNIVERSITY OF
CALIFORNIA

*Radiation
Laboratory*

TWO-WEEK LOAN COPY

*This is a Library Circulating Copy
which may be borrowed for two weeks.
For a personal retention copy, call
Tech. Info. Division, Ext. 5545*

BERKELEY, CALIFORNIA

DISCLAIMER

This document was prepared as an account of work sponsored by the United States Government. While this document is believed to contain correct information, neither the United States Government nor any agency thereof, nor the Regents of the University of California, nor any of their employees, makes any warranty, express or implied, or assumes any legal responsibility for the accuracy, completeness, or usefulness of any information, apparatus, product, or process disclosed, or represents that its use would not infringe privately owned rights. Reference herein to any specific commercial product, process, or service by its trade name, trademark, manufacturer, or otherwise, does not necessarily constitute or imply its endorsement, recommendation, or favoring by the United States Government or any agency thereof, or the Regents of the University of California. The views and opinions of authors expressed herein do not necessarily state or reflect those of the United States Government or any agency thereof or the Regents of the University of California.

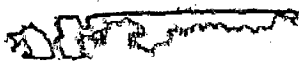
UCRL-2708
Unclassified Instrumentation

UNIVERSITY OF CALIFORNIA
Radiation Laboratory
Berkeley, California
Contract No. W-7405-eng-48

AN ALTERNATING-GRADIENT CHANNEL
USING PERMANENT BAR MAGNETS

Warren Fenton Stubbins

September 3, 1954



Printed for the U. S. Atomic Energy Commission

AN ALTERNATING-GRADIENT CHANNEL
USING PERMANENT BAR MAGNETS

Warren Fenton Stubbins

Radiation Laboratory, Department of Physics
University of California, Berkeley, California

September 3, 1954

ABSTRACT

An alternating-gradient channel for containing relativistic electrons (7 Mev) is made by arranging sets of four permanent bar magnets along an evacuated tube. The resultant field in each set is calculated assuming point magnetic poles. The range of the forcing field linear from the axis of the assembly is determined. The criteria for magnet strengths and set positions are determined. Experimental results of a system are stated.

AN ALTERNATING-GRADIENT CHANNEL USING PERMANENT BAR MAGNETS

Warren Fenton Stubbins

Radiation Laboratory, Department of Physics
University of California, Berkeley, California

September 3, 1954

I. INTRODUCTION

The use of permanent bar magnets as the source of the magnetic field for an alternate-gradient focusing system has been proposed before.¹ The use of permanent magnets has the advantages of requiring no power supply and consequent attention, and the possibility of being used in confined regions such as drift tubes. The system is limited to the strength of the magnetic poles and the field produced. The addition of pole tips to bar magnets or the magnetization of formed pieces may offset this limitation.

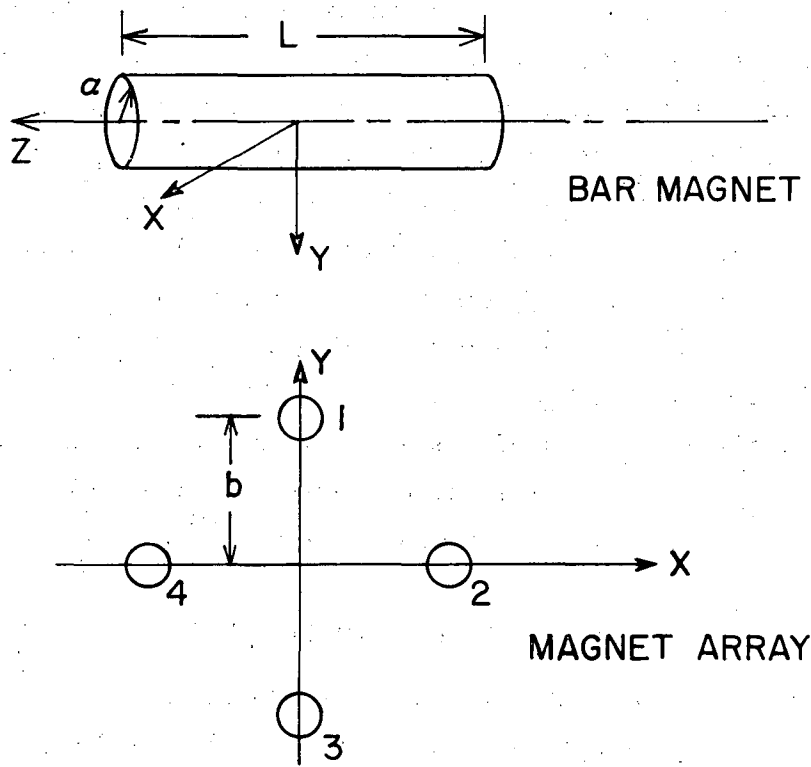
This paper considers the use of four cylindrical bar magnets per set without the addition of pole tips. Three- to 7-Mev electrons are to be confined by the alternate-gradient fields as they drift in an evacuated tube 10 feet long. The entrance aperture and the exit aperture are both 5/8 in. in diameter, with the divergence at the entrance aperture 10^{-2} radians.

II. MAGNETIC FIELD FROM FOUR BAR MAGNETS

The magnetic field from four bar magnets arranged as in Fig. 1 may be calculated using the assumption of point poles. The field components normal to the axis of the magnet are given by the following expressions:

$$B_x = \pi a^2 \left\{ M_1 x \left(\frac{1}{[(y-b)^2 + x^2 + (z - \frac{l}{2})^2]^{3/2}} - \frac{1}{[(y-b)^2 + x^2 + (z + \frac{l}{2})^2]^{3/2}} \right) \right. \\ \left. + M_2 (x-b) \left(\frac{1}{[(x-b)^2 + y^2 + (z - \frac{l}{2})^2]^{3/2}} - \frac{1}{[(x-b)^2 + y^2 + (z + \frac{l}{2})^2]^{3/2}} \right) \right\}$$

¹Clogston and Heffner, J. Appl. Phys. 25, 436 (1954)



MU-8315

Fig. 1

$$\begin{aligned}
 & + M_3 x \left(\frac{1}{\left[(y+b)^2 + x^2 + (z-\frac{\ell}{2})^2 \right]^{3/2}} - \frac{1}{\left[(y+b)^2 + x^2 + (z+\frac{\ell}{2})^2 \right]^{3/2}} \right) \\
 & + M_4 (x+b) \left(\frac{1}{\left[(x+b)^2 + y^2 + (z-\frac{\ell}{2})^2 \right]^{3/2}} - \frac{1}{\left[(x+b)^2 + y^2 + (z+\frac{\ell}{2})^2 \right]^{3/2}} \right) \Bigg\} , \\
 B_y = \pi a^2 & \left\{ M_1 (y-b) \left(\frac{1}{\left[(y-b)^2 + x^2 + (z-\frac{\ell}{2})^2 \right]^{3/2}} - \frac{1}{\left[(y-b)^2 + x^2 + (z+\frac{\ell}{2})^2 \right]^{3/2}} \right) \right. \\
 & + M_2 y \left(\frac{1}{\left[(x-b)^2 + y^2 + (z-\frac{\ell}{2})^2 \right]^{3/2}} - \frac{1}{\left[(x-b)^2 + y^2 + (z+\frac{\ell}{2})^2 \right]^{3/2}} \right) \\
 & + M_3 (y+b) \left(\frac{1}{\left[(y+b)^2 + x^2 + (z-\frac{\ell}{2})^2 \right]^{3/2}} - \frac{1}{\left[(y+b)^2 + x^2 + (z+\frac{\ell}{2})^2 \right]^{3/2}} \right) \\
 & \left. + M_4 y \left(\frac{1}{\left[(x+b)^2 + y^2 + (z-\frac{\ell}{2})^2 \right]^{3/2}} - \frac{1}{\left[(x+b)^2 + y^2 + (z+\frac{\ell}{2})^2 \right]^{3/2}} \right) \right\} ,
 \end{aligned}$$

where a is the radius of the magnets, ℓ is their length, b is their distance from the axis of the assembly, and M_1, M_2, M_3, M_4 are the pole strengths of the respective magnets. One may choose M positive for a north pole and negative for a south pole.

The field component B_x was computed for the plane of the poles at $x = \ell/2$ and is shown in Fig. 2. The magnets considered were $\ell = 5$ in. long with $b = 2.35$ in., and the odd poles were chosen positive and the even ones negative.

That value of the x component along the $y = 0$ axis is consistently larger than along the $x = y$ axis does not imply an asymmetry in the system. The impulse must be calculated over the path $z = 0$ to ∞ . The field value for this path is shown in Fig. 3. The integral of this curve is the impulse given to the particle as it passes from the center of the magnet array outward.

The impulse was computed for several values of particle displacement from the axis and the linearity is quite good, as shown in Fig. 4. The

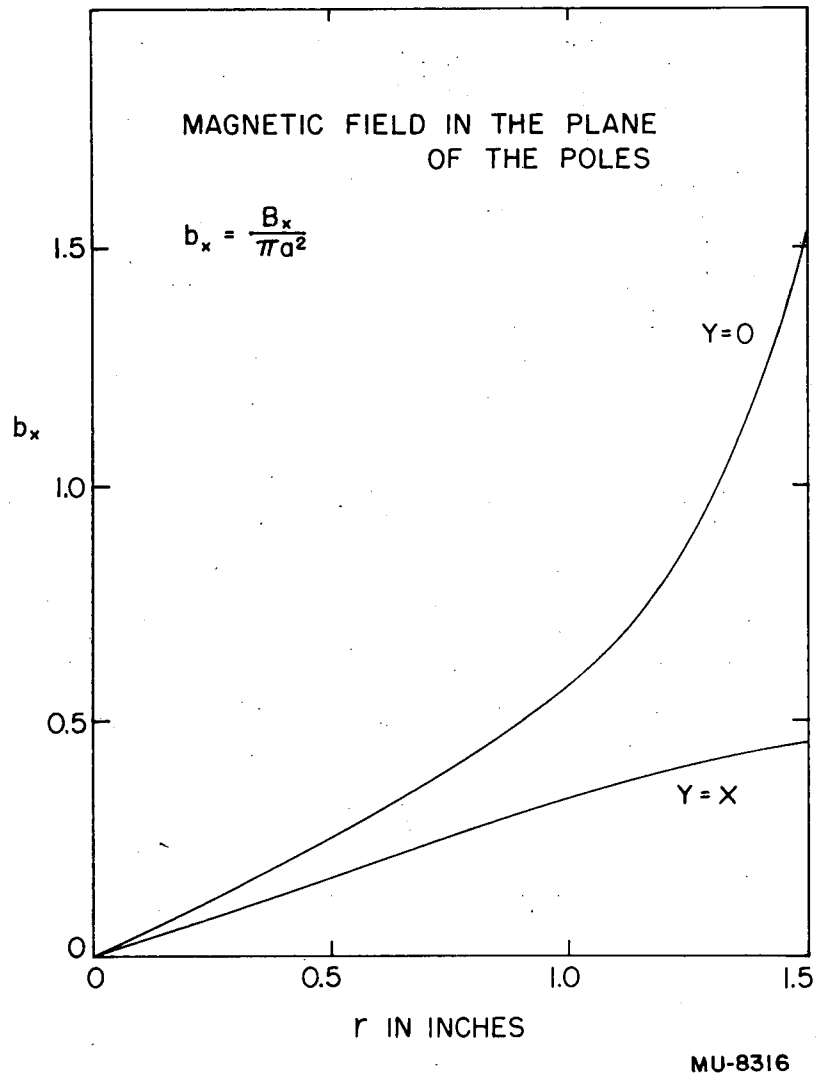
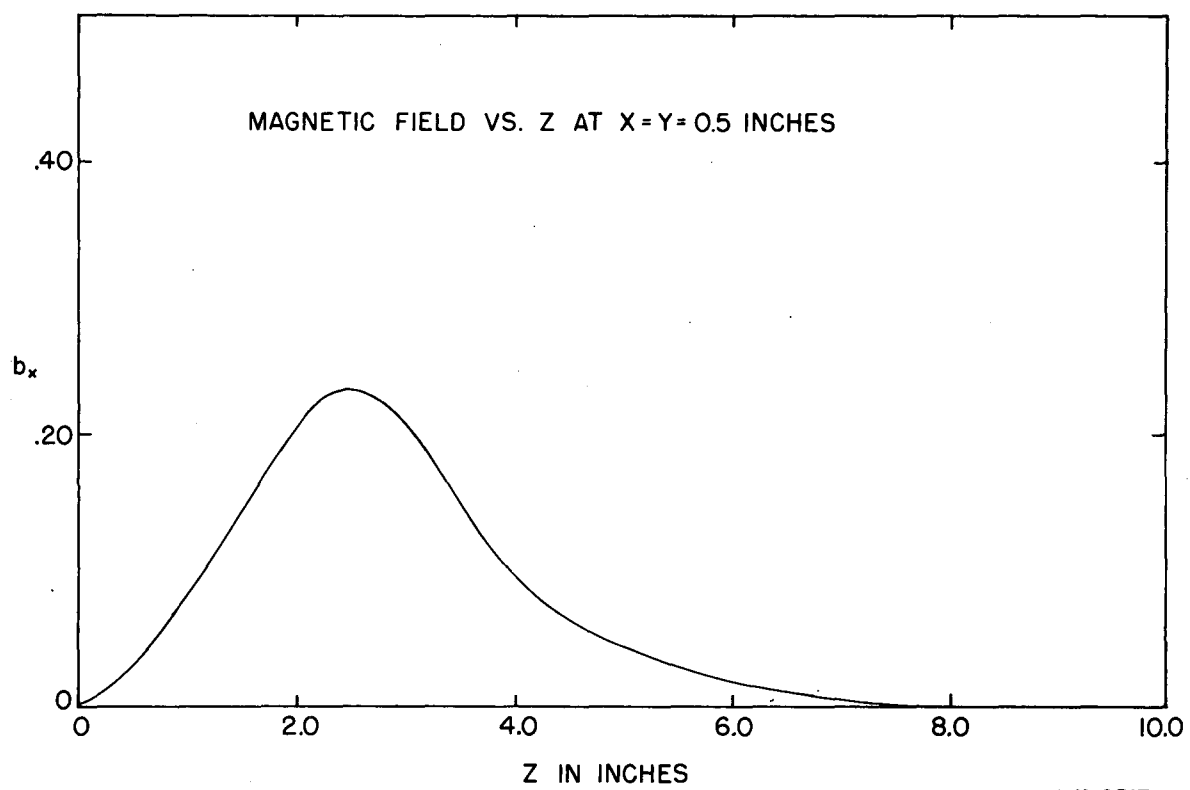


Fig. 2



MU-8317

Fig. 3

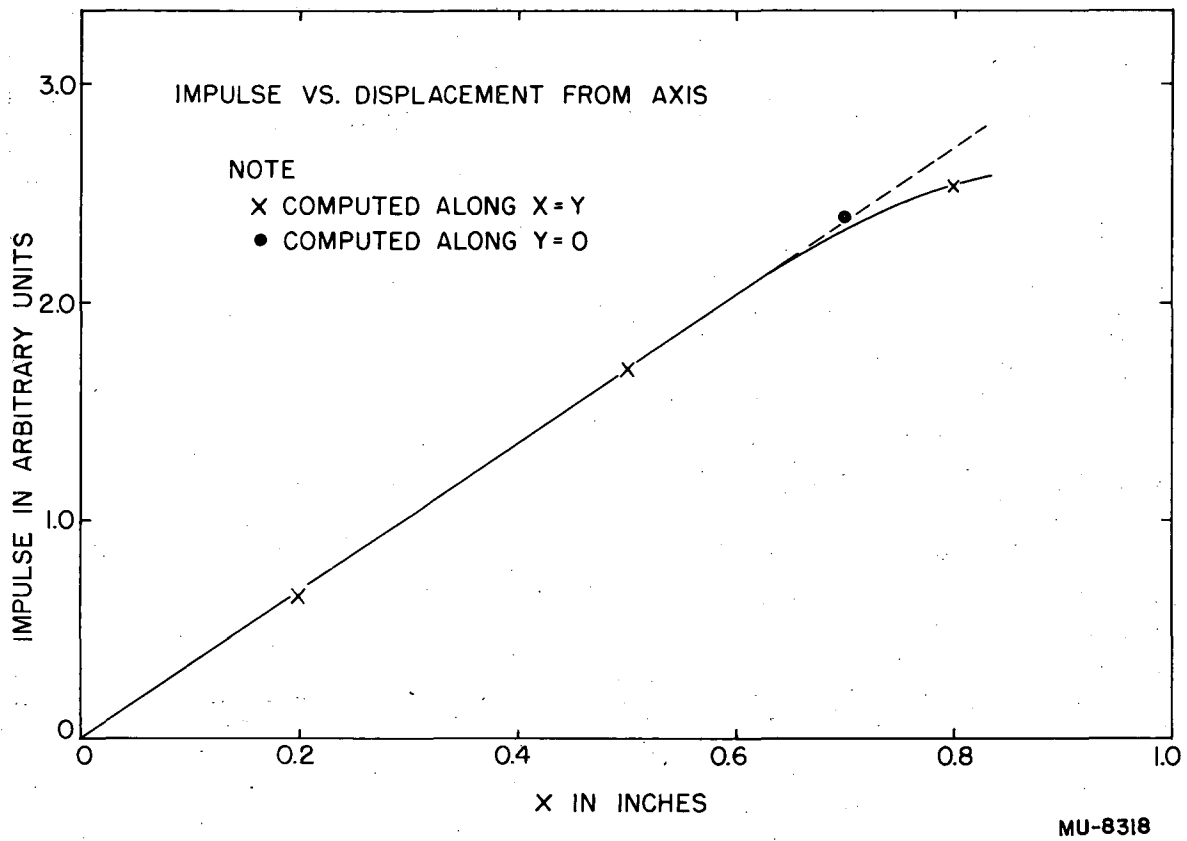


Fig. 4

68-4

impulse is a linear function of the displacement from the axis for the two planes, $x = y$ and $y = 0$ to values of $x = 0.7''$.

Figure 5 shows the field computed when the magnet sets are placed in a series as shown in Fig. 6a and 6b. The equivalent square wave, which has the same impulse, is shown also in Fig. 5. In case 6a the repeat length is $2l = 10$ inches, while in case 6b it is $4l = 20$ inches.

The use of equivalent square waves simplifies the computation below. Included in this approximation is the tacit assumption that the particles do not change their axial displacement appreciably during the time they receive the impulse.

The advantage of case 6b over 6a in the required magnetic pole strength is shown below. The required pole strength is approximately one-fourth as much for the long-period arrangement. Further reductions in pole strength requirements are made for cases 6c and 6d.

III. EQUATIONS OF MOTION IN THE FIELDS

The force on a charged particle moving in a magnetic field is given by the Lorentz equation,

$$F = \frac{+e}{c} \vec{v} \times \vec{B}.$$

The fields we calculated above are normal to the velocity of the electrons. Thus we may consider the scalar equation

$$F = m \frac{d^2 x}{dt^2} = \frac{-e}{c} |v| |B|.$$

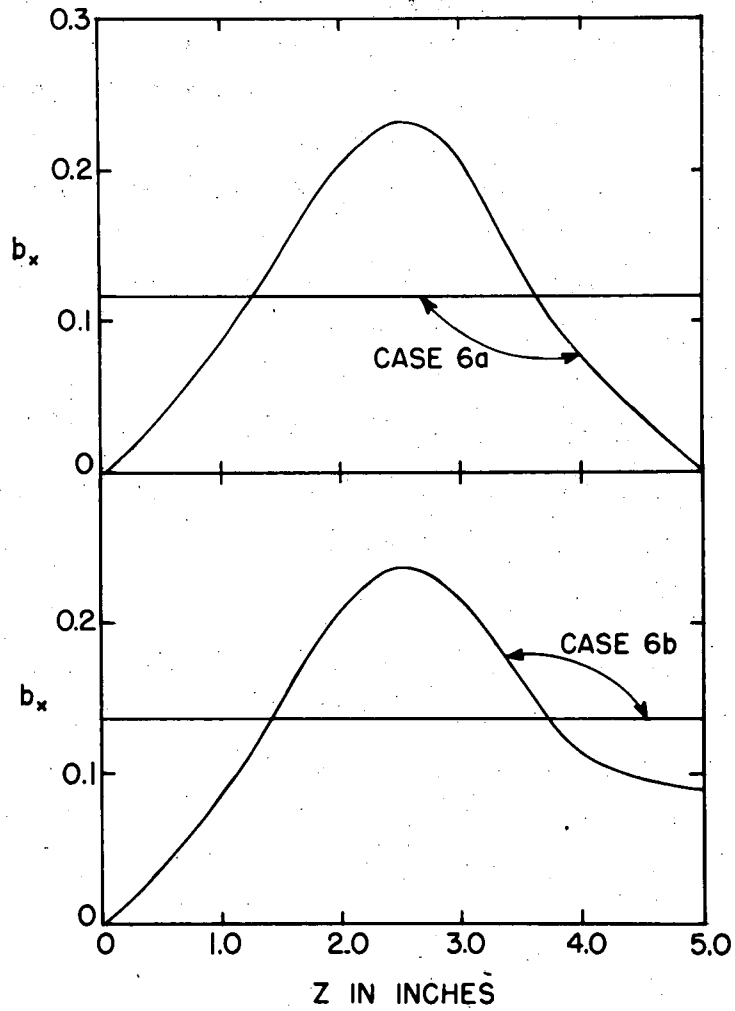
Since these electrons are highly relativistic, $v \doteq c$, and since $v = dz/dt$ in our system, if we let $B = \frac{\partial B}{\partial x} x$ the equation becomes

$$\frac{d^2 x}{dz^2} + \frac{e}{mc^2} \frac{\partial B_x}{\partial x} x = 0.$$

Since $mc^2 = E$, the total energy of the particle, and we note that

$$\frac{e}{E} \frac{\partial B}{\partial x} = \omega^2,$$

MAGNET FIELD VS. Z FOR CASES 6a & 6b
SHOWING EQUIVALENT SQUARE PULSE



MU-8319

Fig. 5

ARRANGEMENT OF MAGNET SETS AND EQUIVALENT FIELDS

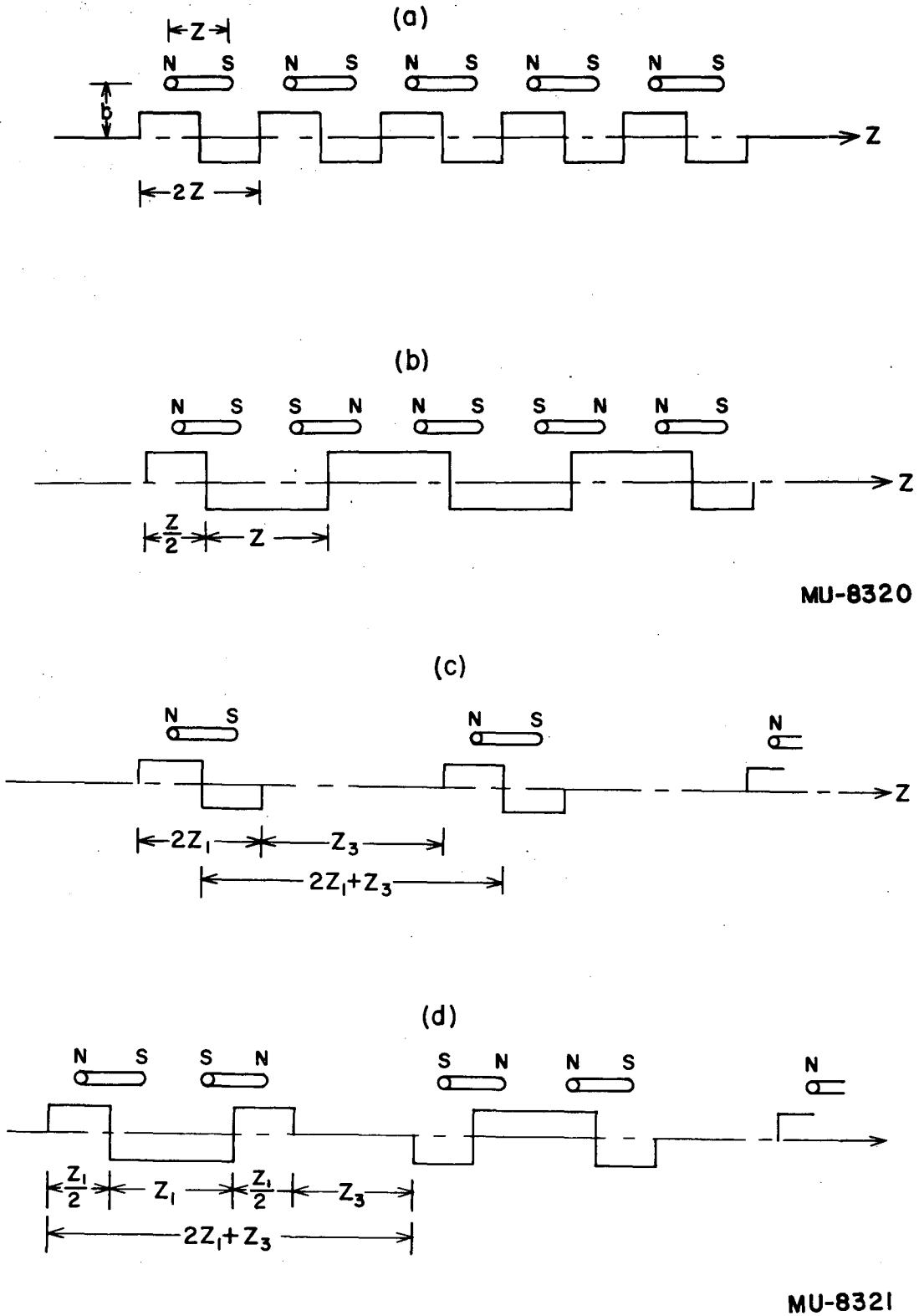


Fig. 6

we have $\frac{d^2x}{dz^2} + \omega^2 x = 0$ as the equation of motion of the particles in the region of the fields. Since $\frac{\partial B}{\partial x}$ changes sign periodically, the equation may be either stable or unstable, depending upon the sign of ω^2 . In the stable region the two independent solutions are a sine and a cosine, and in the unstable region they are a hyperbolic sine and a hyperbolic cosine.

Choosing an initial displacement and slope and using the two independent solutions, we may obtain the values of the displacement and slope at any later time:

$$\left. \begin{aligned} x &= x_0 \cos \omega_1 z + \frac{1}{\omega_1} \dot{x}_0 \sin \omega_1 z \\ \dot{x} &= -x_0 \omega_1 \sin \omega_1 z + \dot{x}_0 \cos \omega_1 z \end{aligned} \right\} \begin{array}{l} \text{in stable} \\ \text{regions;} \end{array}$$

$$\left. \begin{aligned} x &= x_0 \cosh \omega_2 z + \frac{1}{\omega_2} \dot{x}_0 \sinh \omega_2 z \\ \dot{x} &= x_0 \omega_2 \sinh \omega_2 z + \dot{x}_0 \cosh \omega_2 z \end{aligned} \right\} \begin{array}{l} \text{in unstable} \\ \text{regions.} \end{array}$$

These may, for particular convenience in this problem, be expressed in matrix form:

$$\begin{pmatrix} x \\ \dot{x} \end{pmatrix} = \begin{pmatrix} \cos \omega_1 z, & \frac{1}{\omega_1} \sin \omega_1 z \\ -\omega_1 \sin \omega_1 z, & \cos \omega_1 z \end{pmatrix} \begin{pmatrix} x_0 \\ \dot{x}_0 \end{pmatrix} \quad \begin{array}{l} \text{in stable} \\ \text{region;} \end{array}$$

$$\begin{pmatrix} x \\ \dot{x} \end{pmatrix} = \begin{pmatrix} \cosh \omega_2 z, & \frac{1}{\omega_2} \sinh \omega_2 z \\ \omega_2 \sinh \omega_2 z, & \cosh \omega_2 z \end{pmatrix} \begin{pmatrix} x_0 \\ \dot{x}_0 \end{pmatrix} \quad \begin{array}{l} \text{in unstable} \\ \text{region.} \end{array}$$

For passage through a focusing and then a defocusing region, the product of the matrices applies, and allowing $\omega_1 = \omega_2 = \omega$ we obtain:

$$\begin{aligned}
 \begin{pmatrix} x \\ \dot{x} \end{pmatrix} &= \begin{pmatrix} \cosh \omega z, & \frac{1}{\omega} \sinh \omega z \\ \omega \sinh \omega z, & \cosh \omega z \end{pmatrix} \begin{pmatrix} \cos \omega z, & \frac{1}{\omega} \sin \omega z \\ -\omega \sin \omega z, & \cos \omega z \end{pmatrix} \begin{pmatrix} x_0 \\ \dot{x}_0 \end{pmatrix} \\
 &= \begin{pmatrix} \cos \omega z \cosh \omega z - \sin \omega z \sinh \omega z, & \frac{1}{\omega} (\sin \omega z \cosh \omega z + \cos \omega z \sinh \omega z) \\ \omega \cos \omega z \sinh \omega z - \omega \sin \omega z \cosh \omega z, & \sin \omega z \sinh \omega z + \cos \omega z \cosh \omega z \end{pmatrix} \\
 &\quad \cdot \begin{pmatrix} x_0 \\ \dot{x}_0 \end{pmatrix} \\
 &= \begin{pmatrix} A & B \\ C & D \end{pmatrix} \begin{pmatrix} x_0 \\ \dot{x}_0 \end{pmatrix}
 \end{aligned}$$

For stability over one cycle it may be shown² that

$$\left| \frac{A + D}{2} \right| < 1.$$

The most stable condition appears to lie midway between these limits; i. e.,

$$\frac{A + D}{2} = 0.$$

For configuration as shown in Fig. 6c, where there is a drift space between the region of fields, an additional matrix may be multiplied in to account for this region. This matrix may be formed from either of the initial ones by setting $\omega = 0$; i. e., $\frac{\partial B}{\partial x} = 0$. One obtains

$$\begin{pmatrix} 1 & z_3 \\ 0 & 1 \end{pmatrix},$$

where z_3 is the length between magnet fields.

²L. A. Pipes, J. Appl. Phys. 24, 902 (1953)

For cases 6a and 6b,

$$\left| \frac{A + D}{2} \right| = \left| \cos \omega z \cosh \omega z \right| < 1,$$

and for the optimum case, $\omega z = \frac{\pi}{2} (2n + 1)$. Using the lowest-order case, $n = 0$, we have

$$\begin{aligned} \omega z &= \frac{\pi}{2} \\ \omega^2 &= \frac{\pi^2}{4} \frac{1}{z^2} \\ &= \frac{e}{E} \frac{\partial B}{\partial x}, \end{aligned}$$

thus we obtain the optimum field gradient

$$\frac{\partial B}{\partial x} = \frac{\pi^2}{4} \frac{E}{e} \frac{1}{z^2}$$

As an example we consider two cases for 6.7-Mev electrons:

Case 6a $z = 5$ in. $\frac{\partial B}{\partial x} = 342$ gauss/cm,

Case 6b $z = 10$ in. $\frac{\partial B}{\partial x} = 85.5$ gauss/cm.

By reference to case 6a we find $\frac{\partial B}{\partial x} = \frac{0.232}{2.54} (\pi a^2 M)$ and obtain a value for M required. It is more informative to specify the field required at a point near an isolated bar magnet. Using the first term in the expression for B_x above, with the condition $y = b$ and a measured field at a position x and $z = l/2$, one may specify the strength of the pole of the measured magnet. By comparing pole strengths, one obtains the field value that must be achieved in magnetizing the magnets for the system.

For the case 6c, the matrix becomes

$$\begin{aligned} \begin{pmatrix} x \\ \dot{x} \end{pmatrix} &= \begin{pmatrix} 1 & 2_3 \\ 0 & 1 \end{pmatrix} \cdot \begin{pmatrix} A & B \\ C & D \end{pmatrix} \cdot \begin{pmatrix} x_0 \\ \dot{x}_0 \end{pmatrix} \\ &= \begin{pmatrix} A' & B' \\ C' & D' \end{pmatrix} \begin{pmatrix} x_0 \\ \dot{x}_0 \end{pmatrix} \end{aligned}$$

and we require $\left| \frac{A' + D'}{2} \right| < 1$, which means

$$\left| \cos \omega z \cosh \omega z + \frac{\omega z_3}{2} (\cos \omega z \sinh \omega z - \sin \omega z \cosh \omega z) \right| < 1.$$

For optimum we set this equal to zero and obtain

$$\frac{z}{\omega z_3} = \tan \omega z - \tanh \omega z.$$

For a configuration of 4-inch-long bar magnets (shorter than those considered earlier, but whose field form is assumed the same, almost symmetrical about the ends of the bar), which will cover ten feet evacuated tube with 8 sets of magnets, the following analysis applies:

$$z_1 = z_2 = z = 4 \text{ in.},$$

$$z_3 = 7 \text{ in.}$$

Table I

ωz	ω	$\frac{\partial B}{\partial x} \frac{\text{gauss}}{\text{cm}}$	$z_3 \text{ cm}$	$z_3 \text{ inches}$
0.9	0.0885	175	41.5	16.4
1.0	0.0985	216	25.6	10.0
1.1	0.1082	260	15.9	6.2
1.2	0.118	310	9.8	3.9
1.3	0.128	366	5.7	2.2
1.4	0.1375	422	2.9	1.1

Thus for 7 in. = z_3 , $\omega z = 1.08 \text{ rad} = 61^\circ 53'$

$$\frac{\partial B}{\partial x} = 252 \text{ gauss/cm}$$

For the configuration of Fig. 6d the criteria for stability may also be determined by requiring the trace of the matrix computed over a complete cycle to be less in absolute magnitude than 2. Because the period includes so many steps the expression is more complicated. Again, if the trace is set equal to zero the most stable arrangement is achieved. This occurs when the roots of the following equation are satisfied by (ωz_3) .

$$\begin{aligned}
T = (z_3 \omega)^2 & \left[\sin^2 \omega z_1 \cosh \omega z_1 + \sinh^2 \omega z_1 \cos \omega z_1 - \sin \omega z_1 \sinh \omega z_1 \right. \\
& \left. - \sinh \omega z_1 \cosh \omega z_1 \sin \omega z_1 \cos \omega z_1 \right] \\
+ 2 (z_3 \omega) & \left[\sinh \omega z_1 \cosh \omega z_1 \cos^2 \omega z_1 - \sin \omega z_1 \cos \omega z_1 \cosh \omega z_1 \right. \\
& \left. - \cos \omega z_1 \sin \omega z_1 \cosh^2 \omega z_1 + \sinh \omega z_1 \cosh \omega z_1 \cos \omega z_1 \right] \\
+ 2 & \left[\cos^2 \omega z_1 \cosh^2 \omega z_1 + \cos \omega z_1 \sinh^2 \omega z_1 - \cosh \omega z_1 \sin^2 \omega z_1 \right] = 0.
\end{aligned}$$

Figure 7 shows the relation between ω and z_3 for the optimum condition and the bounds of stability. Recalling that ω depends upon the particle energy, one may determine the range of energy for which a configuration is stable by inspection of the figure.

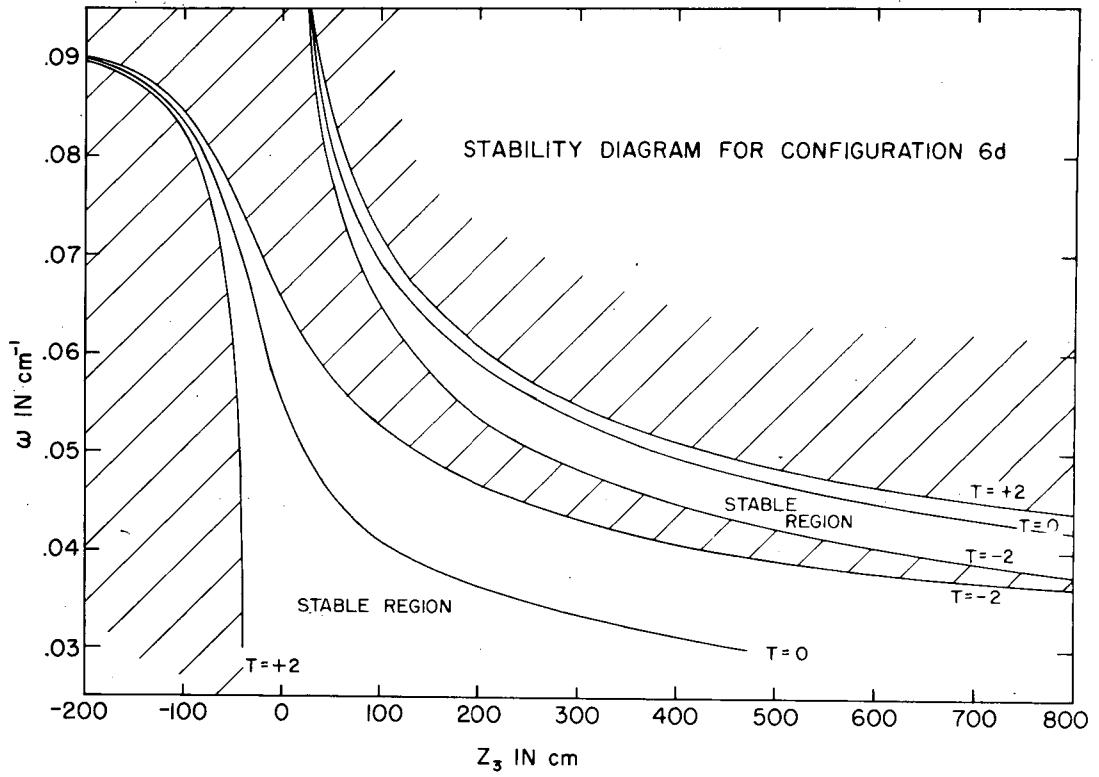
IV. ADJUSTMENTS TO THE SYSTEM

In magnetizing the bar magnets, the proper magnetization procedure will insure the least change in the field values after installation due to aging and the presence of adjacent magnets. It is recommended that the magnets be fully magnetized by placing them in a solenoid. After the removal of the magnetizing field, demagnetization may be accomplished either by the solenoid or by the use of additional bar magnets. Care then should be taken to keep the magnets at least as far apart as they will be in their holders, to avoid further demagnetization.

Variations in the magnetic pole strengths of a few percent may occur in the magnetization process. Magnets for each set should be chosen with as small a variation as possible in their pole strengths.

The optimum adjustments for a particular pole strength and electron energy may be made as follows in the arrangement of Fig. 6c:

- (a) To simulate a weaker pole strength, i. e., lower gradient, reduce the separation between magnet sets (see Table I).
- (b) To simulate a stronger pole strength, lengthen the spacing between sets.
- (c) To optimize for a higher-energy electron, increase the spacing between magnets.



MU-8322

Fig. 7

- (d) To obtain a focus for a particle of given energy near the end of the magnetic array, either increase or decrease the separation between sets.
- (e) To increase the effect of a given pole strength, increase the period of the alternating gradient by pairing adjacent magnet sets.

The assistance of Mrs. Bonnie Gronlund and Messrs. Aram Thomasian and James Baker in making many calculations is greatly appreciated.

V. EXPERIMENTAL RESULTS

Eight sets of bar magnets were obtained and magnetized to a pole strength that resulted in a field gradient of 100 gauss per centimeter when the magnets were mounted in their holders. To obtain the optimum position for the sets we consider arrangement 6c and the equation

$$\frac{z}{\omega z_3} = \tan \omega z_1 - \tanh \omega z_1.$$

From $\frac{\partial B}{\partial x} = 100$ gauss/cm we obtain $\omega = 0.067 \text{ cm}^{-1}$. For $z_1 = 8 \text{ in.} = 20.4 \text{ cm}$, $\omega z_1 = 1.36 = 78^\circ$. This gives $z_3 = 7.8 \text{ cm} = 3 \text{ in.}$, which gives a value of $2z_1 + z_3 = 19 \text{ in.}$

The measured values of increase in current upon a probe for various arrangements is shown in Table II.

Table II

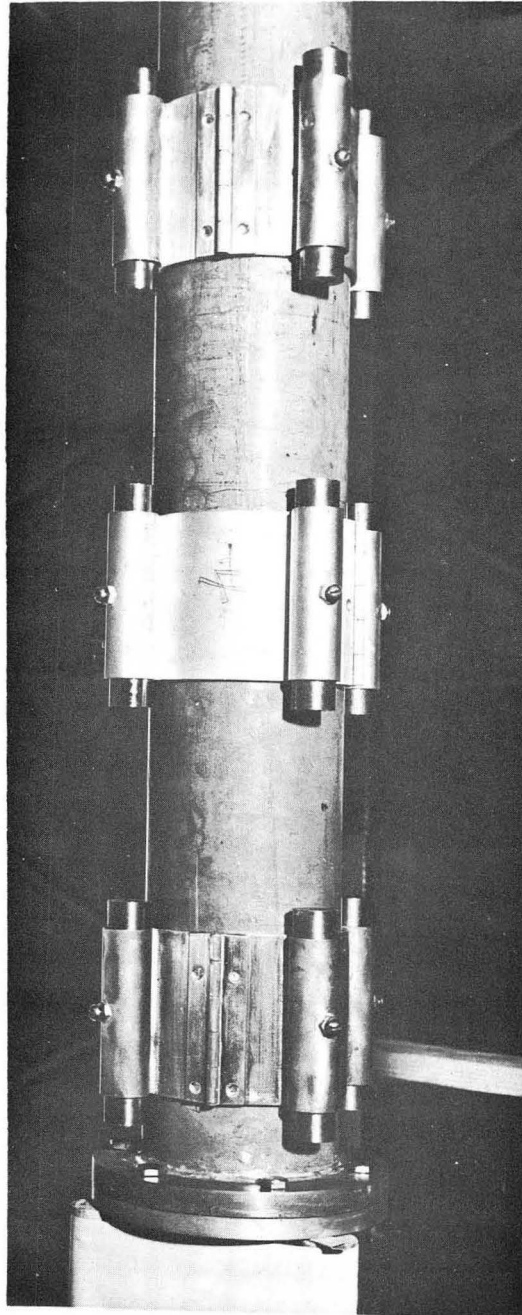
Arrangement	$2z_1 + z_3$	z_1	Multiplication Factor in Probe Current	Distance to Current Probe from last Magnet Set
6d	17	4"	5	30"
6d	18	4"	6	30"
6d	19	4"	5	30"
6d	20	4"	4	30"
6d	18	4"	4	34"
6d	17	4"	5	36"
6d	16	4"	6	38"
6d	16.5	4"	6	37"
6d	16.5	3-1/2"	6	38"
6d	16	3-1/2"	6	39"

Other arrangements, as 6a, 6b, 6c, were tried and found inferior to arrangement 6d with these pole strengths, i. e., $\frac{\partial B}{\partial x} = 100$ gauss/cm.

Inspection of Fig. 7 shows that the optimum values above do not lie at the expected places on the graph. It is believed that the square-wave approximation shown in Fig. 5 is too high, owing to the rapid change in radius of the particles as they move through the system. Trajectory computations show frequent crossovers.

The pattern of the beam observed on a fluorescent screen was a pattée cross with an intense center. The bars of the cross were rotated 45° from the cross formed by planes diametrically through the magnets.

Remagnetizing the bar magnets to twice their initial pole strengths (after taking into account the difference between computed and effective gradient) and arranging them as in Fig. 6b resulted in a 10- to 20-fold increase in current on the target probe. The arrangement is shown in Fig. 8. This is the shortest practical repeat length with the pole strengths available. The excursions of the electrons are minimum under this condition and this



ZN-1041

Fig. 8

contributes to the higher multiplication factor.

This work was done under the auspices of the U. S. Atomic Energy Commission.